Valeria BOSCAINO[1],Rosario MICELI[1],Giuseppe CAPPONI[1],Giuseppe RICCO GALLUZZO[1], Renato RIZZO[2]

University of Palermo (1), University of Naples (2)

Fuel Cell Analytical Modeling: solving the trade-off between accuracy and complexity

Abstract. *In this paper, a 5.5 kW Proton Exchange Membrane fuel cell is modeled. The proposed analytical model is described and the parameters identification procedure is further discussed. Simulation results of all three sub-models are compared to test the accuracy of each one. A comparison between simulation and experimental results is provided as well validating the modeling approach.*

Streszczenie. *W pracy przedstawiono model 5.5 kW baterii pracującej na zasadzie membrany protonowej. Przedyskutowano model oraz parametry identyfikacyjne. (**Model baterii z membraną protonową – wybór między dokładnością a złożonością**)*

Keywords: modeling, fuel cell, proton exchange membrane fuel cell, hydrogen.
Słowa kluczowe: bacteria z membrane protonową, modelowanie.

Introduction

In the last few years, a growing attention to efficiency in power conversion, energy saving and renewable energy sources have been highlighted. Several innovative applications appear promoting complete mobility for electric vehicles and handheld devices [1-3]. Yet, state-of-art is not so mature to spread innovative technologies on the market. Wireless power transfer is the key representative of such applications. Research is actually focused on efficiency-related issues [4-8]**.**

Among renewable sources, fuel cells are the most promising source of energy due to their extremely low environmental impact. In the literature, fuel cell-based power supplies are widely presented. Household appliances, automotive and handheld devices are only a few applications [9-16]. In spite of the great advantages brought by fuel cells, hydrogen production and storage related problems must be solved for a successful marketing of fuel cell–based systems. Innovation on fuel cell technology is therefore highly supported by several research programs within and beyond the European Union. Even concerning quite different scientific research areas, fuel cell modelling is a common requirement. A detailed analysis of the electro-chemical and physical behaviour of the fuel cell stack is required by chemical engineers for manufacturing purposes, thus preferring an analytical modelling approach [17-26]. System engineers need to simulate and test the overall system as closely as possible to its effective working conditions, thus preferring an empirical modelling approach [27-32]. Behavioural simulations are commonly used to validate power supply systems to shorten the overall design process, often taking advantage from several co-simulation options [33-36]. Therefore, choosing an analytical or empirical approach is a critical design step.

This paper proposes a steady-state analytical model of a 5.5 kW Nuvera Proton Exchange Membrane (PEM) fuel cell. Several degrees of accuracy are here proposed. Three versions are proposed, each one accounting for a different number of independent parameters: ten-parameters, six-parameters and four-parameters model. The designer can solve the trade-off between the model complexity and accuracy by himself and according to the specific application, taking all the advantages brought by a unique model architecture. A comparison of the accuracy of each sub-model is provided. Simulation and experimental results are compared to test the high performances and reliability of the proposed fuel cell model. The ten-parameters model is the most accurate but the model complexity is quite high. The six-parameters model is the best trade-off between the ten- and four-parameters models. Instead, the four-parameters sub-model features very low complexity and the lowest accuracy.

The ten-parameters model

The ten-parameters model is the most complete of all sub-models. This model features the highest accuracy, as it will be shown by experimental results. The following assumptions are made:

- Instantaneous chemical reactions in the polymeric membrane;
- Ideal reactive gases.

The fuel cell voltage is given by:

$$v_{fc} = E_{Nernst} - v_{act} - v_{ohm} - v_{con} \tag{1}$$

where E_{Nernst}, also-called the Nernst-voltage, is the ideal electro-motive force of the electro-chemical cell. The Nernst voltage which is approximately 1.2V for low-temperature cells is never truly obtained even if an open-circuit condition is considered. As described by (1), irreversible losses at both the cathode and the anode should be accounted for. Multiple phenomena contribute to the irreversible losses. Three losses can be distinguished: activation polarization (v_{act}), ohmic polarization (v_{ohm}), concentration polarization (v_{con}). These losses result in a cell voltage (V) that is less than its ideal potential, E_{Nernst}.

The Nernst voltage can be expressed as:

$$E_{Nernst} = 1.229 - 0.85 \cdot 10^{-3}(T - 298.15) + \\ + 4.3 \cdot 10^{-5} T \cdot \left[\ln\left(p_{H_2}\right) + \frac{1}{2}\ln\left(p_{O_2}\right) \right] \tag{2}$$

where T is the absolute temperature, p_{O_2} is the oxygen pressure, p_{H_2} is the hydrogen pressure.

Activation losses are mainly related to the activation energy which is the required amount to start the chemical reaction. The activation voltage drop is given by:

$$v_{act} = -\xi_1 + \xi_2 T + \xi_3 \ln(C_{O_2}) + \xi_4 T \ln(i_{fc}) \tag{3}$$

where i_{fc} is the fuel cell current, T the absolute temperature and C_{O_2} is the oxygen concentration at the cathode electrode which is given by:

(4) $$C_{O_2} = \frac{p_{O_2}}{5.08 \cdot 10^6 \exp(-498/T)}$$

ξ_1,ξ_2, ξ_3 and ξ_4 as given by (5), (6), (7) and (8), are four model parameters. Initial values have been set from literature [23-24]. A parameters identification procedure has been carried out to minimize the model error.

(5) $$\xi_1 = 0.948$$

(6) $$\xi_2 = 0.00286 + 0.0002 \ln(A) + 4.3 \cdot 10^{-5} \ln(C_{H_2})$$

(7) $$\xi_3 = 7.6 \cdot 10^{-5}$$

(8) $$\xi_4 = -1.93 \cdot 10^{-4}$$

where A is the cell area and C_{H_2} is the hydrogen concentration at the cathode electrode which is given by:

(9) $$C_{H_2} = \frac{p_{H_2}}{RT}$$

The ohmic voltage drop, mainly due to resistance to the electron flow in the bipolar plates is given by:

(10) $$v_{ohm} = i_{fc}(R_m + R_c)$$

where R_m is the resistance to the electron flow through electrodes and R_c the resistance to proton flow through the electrolyte. The ohmic voltage drop is reduced by lowering ohmic resistances. High-conductivity and short-length electrodes should be designed. Further, thin electrodes reduce the proton path thus lowering the proton resistance.

The R_m resistance is given by:

(11) $$R_m = \frac{\rho_m L}{A}$$

where L is the membrane thickness, A the membrane active area. The resistivity ρ_m is given by:

(12) $$\rho_m = \frac{18.61\left[1 + 0.03(i_{fc}/A) + 0.062(T/303)^2 (i_{fc}/A)^{2.5}\right]}{\left[\psi - 0.634 - 3(i_{fc}/A)\right]\exp\left(4.18\frac{T-303}{T}\right)}$$

The exponential term in (12) accounts for an operating temperature different from the nominal one of 30°C.

The reactant which is consumed at the electrode is usually diluted by the reaction products. If high current densities are assumed, the finite mass transport rates limit the supply of fresh reactant and evacuation products. A concentration gradient therefore occurs, contributing to loss of cell potential. The concentration polarization is mainly affected by slow diffusion of reactants and products through the electrolyte. The concentration voltage drop is given by:

(13) $$v_{conc} = -m \exp(ni)$$

where i is the current density, m and n are independent parameters. Initial values have been set from literature [24]. A parameters identification procedure has been carried out to minimize the model error. The m parameter is closely related to the conductivity while the n parameter mainly depends on the porosity of the gases permeation layer. The m parameter accounts for temperature effects, as shown by (14) and (15).

(14) $$m = -1.1 \cdot 10^{-6}(T - 273.15)$$

if T>312.15K

(15) $$m = 3.3 \cdot 10^{-4} - 8.2 \cdot 10^{-5}(T - 273.15)$$

if T<312.15K

The n parameter is equal to:

(16) $$n = 8.3 \cdot 10^{-3}\, cm^2/mA$$

Hydrogen and Oxygen partial pressures are given by:

(17) $$p_{H_2} = p_{H_2O}^{sat}\left[\exp\left(-\frac{1.63 i/A}{T^{1.334}}\right)\frac{p_a}{p_{H_2O}^{sat}} - 1\right]$$

(18) $$p_{O_2} = p_{H_2O}^{sat}\left[\exp\left(-\frac{4.192 i/A}{T^{1.334}}\right)\frac{p_c}{p_{H_2O}^{sat}} - 1\right]$$

where p_a is the anode pressure, p_c the cathode pressure. The water saturation pressure is given by:

(19) $$\log_{10} p_{H_2O}^{sat} = -2.18 + 2.95 \cdot 10^{-2} T_c - 9.18 \cdot 10^{-5} T_c^2 - 1.441 \cdot 10^{-7} T_c^3$$

where T_c is the Celsius operating temperature.

The ten-parameters model includes the cell dynamic behavior. The dynamic response of the fuel cell is modeled by introducing the capacitor C. In PEM fuel cells, the transient response is mainly affected by the charge double-layer phenomenon.

In a PEM fuel cell, the two electrodes are separated by a solid membrane which only allows the H+ ions to pass through, blocking the electron flow. The electrons will flow from the anode through the external load and gather at the surface of the cathode, to which the protons of hydrogen will be attracted at the same time. Thus, two charged layers of opposite polarity are formed across the boundary between the porous cathode and the membrane. The layers, known as electrochemical double layer, can store electrical energy and behave like a supercapacitor.

For example, if the load current suddenly drops to zero level the charge double layer will take some time to disperse and so will the associated overvoltage. However, the ohmic losses which are proportional to the drawn current will immediately reduce to zero. Therefore, the fuel cell response will exhibit an instantaneous drop followed by an exponential decay towards the new steady-state value. The capacitive effect is not affected by ohmic losses. The time-constant is therefore modeled by a capacitor C and equivalent resistances of concentration and activation losses, but not ohmic losses. The time constant is given by:

(22) $$\tau = C(R_{act} + R_{conc})$$

The 5.5 *kW* Nuvera Proton Exchange Membrane Fuel Cell Stack characteristic parameters are listed in Table 1.

The ten parameters are listed in Table 2. The model is implemented and tested in MATLAB/Simulink environment. Simulation and experimental results will be compared to test the high-accuracy of the ten-parameters model.

Table 1. Stack parameters

Parameter	Value
n (number of cells)	40
Cell active area	500 cm^2
Membrane thickness	0.0051 cm
Maximum rated current density	0.4 A/cm^2
Equivalent conductivity of protonic conduction	0.08 S/cm
Maximum rated power	5.5 kW

Table 2. Ten-parameters model coefficients

Parameter	Tuned value
ξ_1	-0.9152
ξ_3	1.79·10-4
ξ_4	$8.692 \cdot 10^{-5}$
c_1	0.0173
c_2	0.00485
c_3	2.8706
c_4	0.6192
c_5	115.4833
ψ	20.8218
n	$9 \cdot 10^{-3}$

Six-parameters model

The six-parameters sub-model is based on the following assumption: instantaneous chemical reactions in the polymeric membrane; constant operating temperature; constant pressure of reactants.

Therefore, the six-parameters sub-model is based on the ten-parameters model neglecting temperature and pressure effects on the fuel cell stack performances. The unavoidable loss in accuracy is therefore counterbalanced by the lower complexity of the proposed sub-model. Following the above mentioned assumption, the activation overvoltage is given by:

$$v_{act} = A \ln\left(\frac{i}{i_o}\right) \tag{20}$$

where A is a constant given by:

$$A = \frac{RT}{2\alpha F} \tag{21}$$

where R is the universal gas constant, F the Faraday constant and α is the charge transmission coefficient whose value depends on the reaction type and electrodes material. From (21) it is worth noting that higher temperatures correspond to higher values of the A parameter and therefore higher values of the activation drop. The ohmic voltage drop is given by:

$$v_{ohm} = R_{ohm} i_{fc} \tag{22}$$

With regards to the ohmic resistance, it could be demonstrated that the internal resistance depends on the cell conductivity σ_m according to:

$$R_{ohm} = \frac{t_m}{\sigma_m} \tag{23}$$

where t_m is the membrane thickness. The conductivity can be expressed as:

$$\sigma_m = b_1 \exp\left[b_2\left(\frac{1}{303} - \frac{1}{T_{fc}}\right)\right] \tag{24}$$

where b_2 is empirically obtained and b_1 is given by:

$$b_1 = b_{11}\lambda - b_{12} \tag{25}$$

where b_{11} and b_{12} are empirical parameters and λ is the stoichiometric speed. According to (23), (24) and (25), the internal resistance is given by:

$$R_{ohm} = \frac{t_m}{b_1 \exp\left[b_2\left(\frac{1}{303} - \frac{1}{T_{fc}}\right)\right]} \tag{26}$$

The concentration drop is modelled by:

$$v_{con} = i\left(c_2 \frac{i}{i_{\max}}\right)^{c_3} \tag{27}$$

where c_2 and c_3 parameters depend on temperature and pressure operating conditions, i is the current density and i_{max} the maximum allowable current density value. The parameter c_2 is obtained by the following relationship:

$$c_2 = (7.16 \cdot 10^{-4} T_{st} - 0.622)\left(\frac{p_{O_2}}{0.1173} + p_{sat}\right) + (1.68 - 1.45 \cdot 10^{-3} T_{st}) \tag{28}$$

if $\frac{p_{O_2}}{0.1173} + p_{sat} < 2atm$

or by:

$$c_2 = (8.66 \cdot 10^{-5} T_{st} - 0.068)\left(\frac{p_{O_2}}{0.1173} + p_{sat}\right) + (0.54 - 1.6 \cdot 10^{-4} T_{st}) \tag{29}$$

if $\frac{p_{O_2}}{0.1173} + p_{sat} > 2atm$.

The saturation pressure is evaluated by:

$$p_{sat} = 1.508 \cdot 10^{-6} T_{st}^4 - 0.0018 T_{st}^3 - 179.6 T_{st}^2 + 1.428 \cdot 10^4 \tag{30}$$

All parameters of the six-parameters sub-model are listed in Table 3.

Table 3. Six-parameter model coefficients.

Parameter	Tuned value
A	1.898
b_{11}	0.0093
b_{12}	0.0028
b_2	391.466
Λ	18.1466
c_3	1.3787

Four-parameters model

The four-parameters sub-model features the lowest complexity. The sub-model is based on the assumption:

- Uniform distribution of reactant gases;
- Constant temperature;
- Constant pressure;
- Resistance is independent of the cell temperature.

The sub-model is based on the equations:

$$v_{act} = b \ln\left(\frac{i_{fc}}{i_o}\right) \tag{31}$$

(32) $$v_{ohm} = R_{ohm} i_{fc}$$

(33) $$v_{conc} = K_1 i_{fc} e^{K_2 i_{fc}}$$

Four parameters are listed in Table 4.

Table 4. Four-parameters model coefficients.

Parameter	Tuned value
b	0.0696
K_1	0.0417
K_2	0.1101
R_{ohm}	0.0001275

Simulation results

A 5.5kW Nuvera PEM fuel cell stack is modelled. The stack is made up of 40 cells which are connected in series. Assuming a uniform behaviour of all elementary cells, the output of the fuel cell stack is obtained by summing the output of each fuel cell model. As an example, in Fig.1. the top level model of the ten-parameters model implemented in MATLAB is shown.

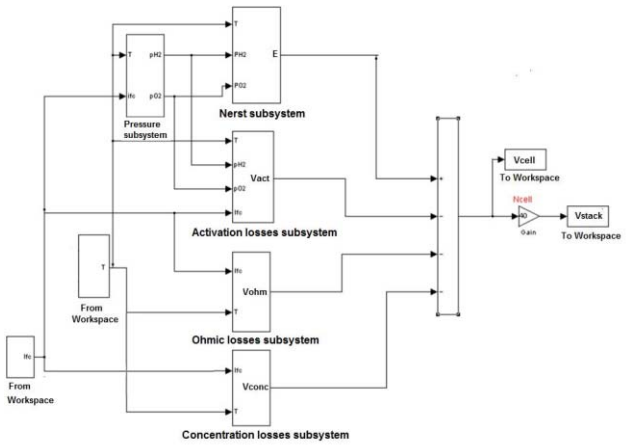

Fig. 1. MATLAB model of the ten-parameters model.

The cell voltage is multiplied by 40 which is the number of active cells of the fuel cell stack under test. Experimental waveform of the fuel cell stack current is forced from MATLAB workspace. The simulated stack voltage is sampled and stored in MATLAB workspace to be compared with the corresponding experimental waveforms.

Model validation

Simulation and experimental results are compared to test the accuracy of each sub-model.

In Figure 2 the averaged iso-themal V-I curve at 30°C and simulated curves of each sub-model are shown. Experimental results are shown by the dotted curve, the ten-parameters model output by the red dashed curve, the six-parameters model by the blue dashed curve and the four-parameters by the pink dashed curve.

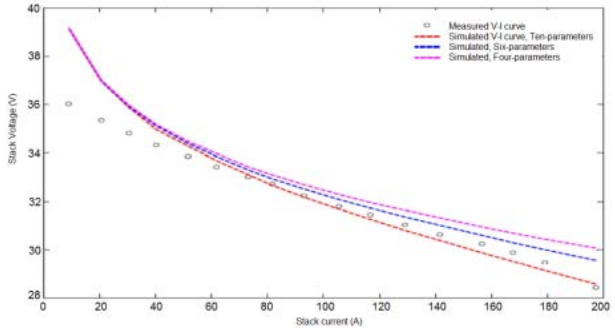

Fig. 2. Experimental and simulated steady-state V-I curves under 30°C.

Deviations of each sub-model from experimental results are shown in Fig. 3. If compared with other sub-models, the ten-parameters model features the highest accuracy. Decreasing the number of independent parameters leads to a decreasing accuracy. Indeed, the deviation is maximum for the four-parameters model.

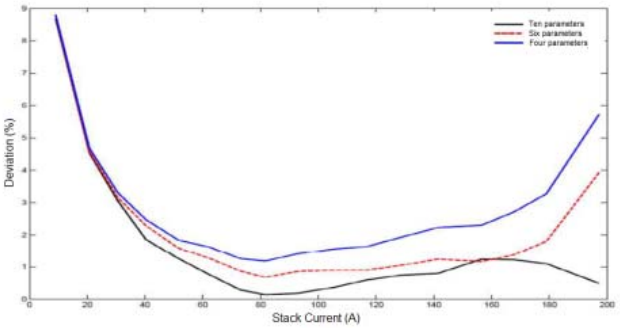

Fig. 3. Standard deviation of proposed analytical models.

The deviation reaches its peak value of 9% in the 0-15A current range, where the activation voltage losses prevail. If the activation polarization region is considered, all deviation curves overlap. If the stack current is higher than 20A, deviation curves split from each other. In the ohmic polarization region, deviation drops to its minimum value. A 2% deviation is achieved by the four-parameters sub-model, a 1% deviation by the six-parameters sub-model while the deviation of the ten-parameters model is really lose to a zero value.

In the concentration polarization region, while the ten-parameters model deviation is less than 1%, the six- and four-parameters sub-models features really high deviation, even beyond 3-4%.

As shown by simulation and experimental results, the deviation from experimental results is lower within the ohmic region. Since in the four-parameters sub-model the proton resistance has been assumed constant, the highest deviation is achieved if compared with other sub-models.

REFERENCES

[1] Brando G., Dannier A., Del Pizzo A., Rizzo R., Power Electronic Transformer for Advanced Grid Management in Presence of Distributed Generation. *International Review of Electrical Engineering IREE*, Vol. 6, n. 7, Dec.2011, ISSN 1827- 6660, pp. 3009-3015.

[2] Rizzo R., Tricoli P., Spina I., An innovative reconfigurable integrated converter topology suitable for distributed generation, *Energies*, Vol. 5, Issue 9, Sept. 2012, ISSN 1996-1073, p. 3640-3654.

[3] Andreotti A., Del Pizzo A., Rizzo R., Tricoli P., An efficient architecture of a PV plant for ancillary service supplying, *International Symposium on Power Electronics Electrical Drives Automation and Motion SPEEDAM*, Pisa, June 2010, pp. 678 – 682.

[4] Miceli R., Energy management and smart grids, *Energies*, 2013, 6 (4), 2262-2290.

[5] Boscaino V., Messina A., Miceli R., Capponi G., Fuel Cells for Household Appliances: experimental test of power management algorithms, *Proc. of the International Conference on Clean Electrical Power ICCEP 2013*, June 2013, 1-6.

[6] Piegari L., Rizzo R., Tricoli P., A Comparison between Line-Start Synchronous Machines and Induction Machines in Distributed Generation, *Prezglad Elektrotechniczny (Electrical Review)*, ISSN 0033-2097, R. 88 n. 5b/2012, pp. 187-193.

[7] Boscaino V., Pellitteri F., La Rosa R., Capponi G., Wireless battery chargers for portable applications: design and test of a high-efficiency power receiver, *Power Electronics IET*, Jan.2013, vol.6, no.1, 20-29.

[8] Boscaino V., Livreri P., Marino F., Minieri M., Current-Sensing Technique for Current-Mode Controlled Voltage Regulator Modules, *Micro-electronics Journal*, Elsevier, 2008, 39, 12, 1852-1859. DOI: 10.1016/j.mejo.2008.05.015.

[9] Liu S., Dougal R.A., Design and Analysis of a Current-Mode Controlled Battery/Ultracapacitor Hybrid, *Proc. IEEE International Conference on Industry Applications*, 3-7 Oct. 2004, 1140-1145.
[10]Gao L., Dougal R.A., Active Power Sharing in Hybrid Battery/Capacitor Power Sources. *Proc. IEEE International Applied Power Electronics Conference*, 9-13 Feb. 2003, 497-503.
[11]Leedy A.W., Nelms R.M, Analysis of a capacitor-based hybrid source used for pulsed load applications, *Proc. IEEE International Energy Conversion Engineering Conf.*, 29-31 July 2002.
[12]Liu S., Dougal R.A., Power Enhancement of an Actively Controlled Battery/Ultracapacitor Hybrid. *IEEE Trans.Power Electronics*, 2005, 20, 236-243
[13]Jiang Z., Dougal R.A., Leonard R.A, Novel Digital Power Controller for Fuel Cell/Battery Hybrid Power Sources. *Proc. IEEE APEC 2005*, 2005, 467-473.
[14]Boscaino V., Collura R., Capponi G., Marino F., A fuel cell–battery hybrid power supply for portable applications. *Proc. 20th International Symposium on Power Electronics, Electrical Drives, Automation and Motion,* Pisa 14-16 June 2010, 580-585.
[15]Jiang Z., Dougal R.A., Synergetic Control of Power Converters for Pulse Current Charging of Advanced Batteries From a Fuel Cell Power Source. *IEEE Trans. on Power Electronics*, 2004, 19, 1140-1150.
[16Jiang Z., Gao L., Dougal R.A., Flexible Multi-objective Control of Power Converter in Active Hybrid Fuel Cell/Battery Power Sources. *IEEE Trans. on Power Electronics*, 2005, 20, 244-253.
[17]Appleby A.J., Foulkes F.R., Fuel Cell Handbook, 6th ed.; *EG&G Technical Services Inc., Science Applications International Corporation, U.S. Department of Energy*, November 2002
[18]Askarzadeh A., Rezazadeh A., An Innovative Global Harmony Search Algorithm for Parameter Identi-fication of a PEM Fuel Cell Model, *IEEE Trans. on Industrial Electronics*, 2010, 59, 3473–3480.
[19]Boscaino V., Miceli R., Capponi G., A semi-empirical multipurpose steady-state model of a fuel cell for household appliances, *Proc. of the International Conference on Clean Electrical Power ICCEP 2013*, June 2013, 1-6.
[20]Chibante R., Campos D., An experimentally optimized PEM fuel cell model using PSO algorithm, *Proc. IEEE International Symposium on Industrial Electronics*, 2010, 2281–2285.
[21]Bonanno D., Genduso F., Miceli R., Main Fuel Cells Mathematical Models: Comparison and Analysis in Terms of Free Parameters, *Proc. of the International Conference on Electrical Machines ICEM 2010*, Rome, 6-8 Sept. 2010, 1-6.
[22]Di Dio V., La Cascia D., Miceli R., Liga R., Integrated mathematical model of proton exchange membrane fuel cell stack (PEMFC) with automotive synchronous electrical power drive, *Proceedings of the IEEE International Conference on Electrical Machines ICEM 2008*, pp.1-6.
[23]Jia J., Li Q., Wang Y., Cham Y.T., Han M., Modeling and Dynamic Characteristic Simulation of a Proton Exchange Membrane Fuel Cell. *IEEE Trans. on Energy Conversion*, 2009, 24, 283-291.
[24]Moreira M.V., Da Silva G.E., A pratical model for evaluting the performance of proton exchange membrane fuel cells, *Journal of Renewable Energy*, 2009, 34, 1734–1741.
[25]Al-Baghdadi, Maher AR. Modelling of proton exchange membrane fuel cell performance based on semi-empirical equations,*Renewable Energy,* 2005, 1587-1599.
[26]Pathapati P.R., Xue X., Tang. J., A new dynamic model for predicting transient phenomena in a PEM fuel cell system,*Renewable energy,*2005, 1-22.
[27]Ramos-Paja C.A, Giral R., Martinez-Salamero L., Romano J., Romero A., Spagnuolo G., A PEM Fuel-Cell Model Featuring Oxygen-Excess-Ratio Estima-tion and Power-Electronics Interaction, *IEEE Trans. on Industrial Electronics*, 2010, 57, 1914-1924.
[28]Chun-Hua, Min, A novel three-dimensional, two-phase and non-isothermal numerical model for proton exchange membrane fuel cell, *Journal of Power Sources*, 2010, 195, 1880–1887.
[29]Boscaino V., Miceli R., Capponi G., Casadei D., Fuel cell modelling and test: experimental validation of model accuracy, *Proc. International Conference on Power Engineering, Energy and Electrical Drives,POWERENG 2013*, 2013, 1–6.
[30]Boscaino V., Miceli R., Capponi G., MATLAB-based simulator of a 5 kW fuel cell for power electronics design, *International Journal of Hydrogen Energy*, Vol. 38, Issue 19, 27 June 2013, 7924-7934.
[31]Boscaino V., Miceli R., Capponi G., A circuit model of a 5kW Fuel Cell, *Proc. International Conference on Clean Electrical Power ICCEP 2013*, June 2013.
[32]Boscaino V., Capponi G., Marino F., FPGA implementation of a fuel cell emulator, *Proc.20th IEEE International Symposium on Power Electronics, Electrical Drives, Automation and Motion*, Pisa, Italy, June 14-16, 2010, 1297-1301.
[33]Bauer P., Korondi P., van Duijsen P.J., Integrated control–Simulation design approach. *Europe 2003, Official proceedings international conferences ZM Communications GmbH*, 227-233.
[34] Boscaino V., Capponi G., Di Blasi G.M., Livreri P., Marino F., Modeling and simulation of a digital design approach for power supply systems. *Proc. IEEE Workshops on Computers in Power Electronics COMPEL 2006*, Troy USA,16-19 July 2006, 246-249.
[35]Di Tommaso A.O., Genduso F., Miceli R., Galluzzo G.R., Computer aided optimization via simulation tools of energy generation systems with universal small wind turbines, *Proc.3rd IEEE International Symposium on Power Electronics for Distributed Generation Systems PEDG 2012*, 570-577.
[36]Ahmed O.A., Bleijs J.A.M., Pspice and Simulink co-simulation for high efficiency DC-DC converter using SLPS interface software, *Proc. IET Intern. Conf. on Power Electronics, Machines and Drives PEMD 2010*, Brighton, 19-21 Apr. 2010, 1-6.

***Authors**: Dr. Valeria Boscaino, Dept. of Energy, Information Eng. and Mathematical models, University of Palermo, viale delle scienze, Palermo, Italy, E-mail: valeria.boscaino@dieet.unipa.it; Prof. Rosario Miceli, Dept. of Energy, Information Eng. and Mathematical models, University of Palermo, viale delle scienze, Palermo, Italy, E-mail: rosario.miceli@unipa.it; Prof. Giuseppe Capponi, Dept. of Energy, Information Eng. and Mathematical models, University of Palermo, viale delle scienze, Palermo, Italy, E-mail: giuseppe.capponi@unipa.it; Prof. Giuseppe Ricco Galluzzo, Dept. of Energy, Information Eng. and Mathematical models, University of Palermo, viale delle scienze, Palermo, Italy, E-mail: giuseppericcogalluzzo@unipa.it; Prof. Renato Rizzo, Dept. of Electrical Enginering and Information Technology, University of Naples, via Claudio 21, Naples, Italy, E-mail: renato.rizzo@unina.it*